Shap. Mem. Superelasticity (2017) 3:192–198
DOI 10.1007/s40830-017-0118-z

SPECIAL ISSUE: ICFSMA 2016, INVITED PAPER

Exploring Magnetic Elastocaloric Materials for Solid-State Cooling

Jian Liu[1,2] · Dewei Zhao[1,2] · Yang Li[1]

Published online: 29 August 2017
© ASM International 2017

Abstract In the past decade, there has been an increased surge in the research on elastocaloric materials for solid-state refrigerators. The strong coupling between structure and magnetism inspires the discovery of new multi-field driven elastocaloric alloys. This work is devoted to magnetic shape memory alloys suitable for mechanical cooling applications. Some novel characteristics in magnetostructural transition materials other than conventional shape memory alloys are overviewed. From the physical and engineering points of view, we have put forward general strategies to maximize elastocaloric temperature change to increase performance reversibility and to improve mechanical properties. The barocaloric effect as a sister-cooling alternative is also discussed.

Keywords Magnetic shape memory alloys · Elastocaloric effect · Magnetostructural transition

Abbreviations

ΔM	Difference of magnetization between martensite and austenite phases (emu/g)
ΔS	Entropy change (J/kgK)
ΔT	Elastocaloric temperature change (K)
T_c	Curie temperature (K)
T_m	Structural transition temperature (K)
H	Magnetic field (T)
δ	Critical stress for martensitic transformation (MPa)
$\Delta\varepsilon$	Transformation strain (%)
m_H	Sensitivity of magnetic field to transformation temperature (T/K)
m_S	Sensitivity of critical stress to transformation temperature (MPa/K)

Introduction

Elastocaloric refrigeration has been recognized as an emerging energy solution to substitute the state-of-the-art vapor compression cooling that not only requires lots of electricity but also is environmentally unfriendly [1]. The principle of elastocaloric effect is to take the latent heat in structural phase transformations by the application of a uniaxial stress [2]. The typical elastocaloric materials are shape memory alloys, such as Ti–Ni [3] and Cu–Zn–Al [4], which exhibit stress-induced reversible martensitic transformation and associated large latent heat. Besides, the elastocaloric effect has been observed in nature rubber [5] and some oxides [6]. As shape memory alloys find a number of advantages (e.g., large potential of cooling capacity, high thermal transfer ability and good fatigue life), they have been suggested to be the preferred regenerates for the current elastocaloric refrigeration systems. Particularly, in magnetic shape memory alloys, the elastocaloric effect that stems from the magnetostructural transformation could be very specific due to the coupling of different degrees of freedom of magnetism and lattice structure. In this unique case, phase transformation characters can be manipulated by the separation or the combination of magnetic and stress fields, through which the

✉ Jian Liu
liujian@nimte.ac.cn

[1] CAS Key Laboratory of Magnetic Materials and Devices, and Zhejiang Province Key Laboratory of Magnetic Materials and Application Technology, Ningbo Institute of Materials Technology and Engineering, Chinese Academy of Sciences, Ningbo 315201, China

[2] University of Chinese Academy of Sciences, 19 A Yuquan Rd, Shijingshan District, Beijing 100049, People's Republic of China

cutting-edge multi-caloric effect is generated [7]. Several comprehensive overviews on conventional elastocaloric alloys and integrated systems are available in the past 2 years [8–12]. The present review paper will emphasis the recent progress in elastocalorics on magnetic shape memory alloys. The strategies to enhance the cooling performance in magnetic shape memory alloys are also discussed.

Magnetic Elastocaloric Materials

Magnetic shape memory alloys can be classified into two sorts: ferromagnetic shape memory alloys (e.g., Ni–Mn–Ga and Ni–Fe–Ga) and metamagnetic shape memory alloys (e.g., Ni–Mn–In and Ni–Mn–Sn). The former one in most cases takes place between two ferromagnetic phases of austenite and martensite. In some cases, the magnetic and structural transitions couple, but this magnetostructural transition is accompanied with a small difference in magnetization ($\Delta M \sim 20$ emu/g) between two phases. So the phase transformation needs to be driven by a relatively large magnetic field. In the late case, the austenite is ferromagnetic, whereas martensite is antiferromagnetic with a large ΔM up to 100 emu/g. This results in an inverse magnetocaloric effect under a lower magnetic field. Studies of elastocaloric effect have been carried out in both classes of magnetic shape memory alloys. In 2010, an independent application of uniaxial stress and magnetic field started in Ni–Mn–Fe–Ga alloys, and the corresponding entropy changes were compared [13]. The elastocaloric effect measured under magnetic field was first studied in 2011 on Ni–Mn–Ga–Co magnetic Heusler shape memory alloys by calculating its isothermal stress-induced entropy change [14]. It is clearly demonstrated that the coupling of uniaxial stress and magnetic field increases both the entropy change and cooling performance, thus supporting the concept of the multi-caloric effect. We recently studied the strength of the magnetostructural interplay in Ni–Mn–Ga–Cu alloys by Landau model, and found that the elastocaloric entropy change accounts for about 53%, while magnetocaloric entropy change about 47% in the total entropy change. In 2013, the combination of elasto- and magnetocaloric effects has been proven to improve the refrigeration capacity of the Ni–Mn–Sn–Cu metamagnetic shape memory alloy [15]. Later on, the direct measurement of adiabatic temperature change (ΔT) was utilized to estimate the elastocaloric properties in Ni–Mn–In–(Co) [16–18], Ni–Fe–Ga–(Co) [19–21], and Ni–Mn–Sn alloys [22]. In order to avoid crack initiation, the input mechanical work is limited for Ni–Mn-based polycrystals. For instance, the applied stress was set less than 150 MPa [17] or applied strain was smaller than 2% [22], with which the martensitic transformation is usually incomplete. Then, a moderate ΔT magnitude of 3–4 K was detected. This elastocaloric effects due to partial transition have surpassed that in ceramics, but lower than those observed in Ti–Ni and Cu–Zn–Al. The lower ΔT also originates from the competition between vibrational term (e.g., +5.5 K in $Ni_{45.7}Mn_{36.6}In_{13.3}Co_{5.1}$) that contributes positively and magnetic part (−2 K) that works against, to the total cooling effect [16]. Nevertheless, when considering the specific ΔT per stress or strain, they are comparable to those observed in thermal shape memory materials, as shown in Fig. 1. As Ni–Fe–Ga alloys are much more ductile, it is possible to driven the higher portion of martensitic phase and achieve higher ΔT. To date, we have discovered an 11 K giant ΔT under a 100 MPa low stress in a Ni–Fe–Ga–Co single crystal, and more importantly it does not show any degradation after 10^4 mechanical cycles [23].

Specifics of Magnetic Materials for Elastocalorics

Magnetically Tuned Transition

The first-order phase transformation is always accompanied by large thermal and stress hysteresis which in most cases strongly prevents functional materials from practical applications, particularly for solid cooling uses. In addition, the functionality of shape memory alloys degrades significantly with cyclic mechanical loadings. Only after a complete transformation on the initial dozens of cycles, the binary Ti–Ni showed a reduced elastocaloric effect by 15%, and then trend to be stabilized in superelasticity and

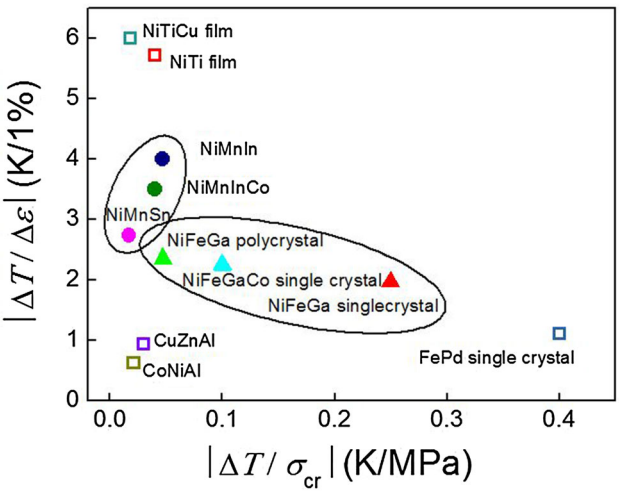

Fig. 1 A comparison of the specific adiabatic temperature change ($|\Delta T/\sigma_{cr}|$ and $|\Delta T/\Delta\varepsilon|$) at room temperature for various elastocaloric materials. *Solid circles* represent Ni_2Mn-based Heusler alloys. *Solid triangles* represent Ni_2FeGa-based Heuslers. The data were taken from Ref. [20] and the related literatures as quoted therein

temperature change [24]. This functional degradation is related to the formation of stressed-transition layers between austenite and martensite phases due to the lattice mismatch. It is proposed to eliminate this stressed-transition layer by making the lattice parameters satisfy the kinematic conditions of compatibility [25]. As demonstrated in a particular $Ti_{54}Ni_{34}Cu_{12}$ thin film with the presence of coherent Ti_2Cu precipitates [26], the functional durability can be strongly improved and does not degrade even after million mechanical cycles. On the other hand, once fixing the optimized composition, the characteristic temperatures and driven stress for martensitic transformation are not easy to change for conventional shape memory alloys. This is unfavorable in a wide cooling span for elastocaloric systems which need cascade refrigerants with tunable transitions. It is true that the temperature window can be widened by means of increasing the applied stress well above the transition, but the engineers prefer to keep a constant stress for the simplicity of cooling machine design and implement.

Magnetostructural transition can be triggered by different stimulus, therefore magnetic field becomes the second option aside from stress. The sensitivity of the driving magnetic field to transformation temperature ($m_H = dH/dT_m$) is a key parameter for the improvement of ΔT in magnetocaloric materials [27]. The m_H value tends to be small at lower magnetostructural transition temperature range, and far from the Curie temperature of austenite, which seems to be closely linked to the nature of first-order transition. The optimization of m_H plays an important role in maximizing ΔT in the finite magnetic field [28]. This argument makes the same sense for elastocaloric effect, as discussed in the following part. Another routine to tune magnetostructural transition in Ni–Mn–(In,Sn) alloys is the variation of the degree of atomic ordering. For instance, T_m in the Ni–Mn–In system is adjustable in 30 K temperature range by an aging processing at 500–600 K, as a result of the effect of the magnetic exchange coupling variations on the free energy difference across martensitic transformation [28, 29].

Lattice Softening

Among numerous magnetic and non-magnetic materials undergoing martensitic transformations, the cubic austenite exhibits the anomaly of pronounced softening of elastic coefficients when approaching T_m. For magnetic shape memory alloys, the most dramatic softening of the TA_2 phonon branch appears around the ferromagnetic ordering temperature due to the strong magnetoelastic coupling. Since the magnetocrystalline anisotropy constant is rather low ($K_{cr} \sim 10^2$ J/m^3 for Ni_2MnGa [30]) and the magnetostriction is relatively large ($\lambda \sim 100$ ppm for Ni_2MnGa [31]), the elasticity in the shear coefficient of C' becomes very unstable affected by temperature or magnetic field [32]. As a result, the Debye temperature varies by the elastic constants according to Launay model [33]. Based on Debye theory, the vibrational entropy can be estimated by

$$S_{vib}(\Theta) = -3Nk_B\ln[1-\exp(-\Theta/T)] + 12Nk_B\left(\frac{T}{\Theta}\right)^3\int_0^{\Theta/T}\frac{x^3dx}{\exp(x)-1}, \quad (1)$$

where N is the number of atoms per mole, k_B is the Boltzmann constant, and Θ is the Debye temperature. From this, a preliminary assumption can be deduced that the vibration entropy change across first-order martensitic transformations should be significant on the second-order Curie transitions (T_c) of austenite. In fact, several experimental results have revealed the maxima ΔS of transformation entropy change when the T_m and T_c are closer [34]. It should be noted that ΔS can be affected by a couple of factors, such as lattice structures, transformation temperature, and magnetoelastic coupling. A high distortion in lattice symmetry normally brings about a higher ΔS as observed in Ti–Ni [35]. Through a comprehensive study on the effect of alloy composition on the latent heat, Frenzel et al. [36] found a linear increase of latent heat with increasing transformation temperature in Ti–Ni-based alloys. In the case of Ni–Mn–Ga magnetic shape memory alloys (Fig. 2), by keeping the same 7 M martensitic structure, we found that the magnetoelastic coupling is a dominate source to the large ΔS, whereas the influence of transformation temperature is less pronounced. Moreover, an abrupt softening in the austenite lattice and corresponding large change in vibrational entropy at T_c was observed in Ni–Mn–In–Co by inelastic neutron scattering measurement [37], suggesting the opportunity of exploiting caloric effects of the second-order transition itself either

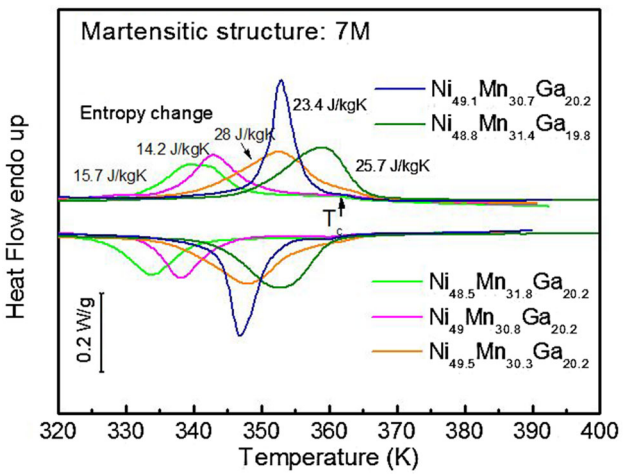

Fig. 2 Calculated entropy changes by differential scanning calorimeter measurements for a set of Ni–Mn–Ga samples with the same 7 M martensitic structures

induced by magnetic field or by stress. This extra part may further enhance the martensitic transformation entropy change and elastocaloric effect [22].

An extreme example of lattice softening is exhibited in Fe–Pd ferromagnetic shape memory alloys. These alloys undergo a second-order-like martensitic transformation with a smeared discontinuity and a small C' less than 1 GPa [38] for austenite (in comparison C about 14 GPa in Ti–Ni [39]). Even in martensitic state, the softening of C' was reported. Consequently, the large elastocaloric effect of 3 K was reported for both austenite and martensite in Fe–Pd single crystals [40, 41]. The most highlight in Fe–Pd is that the origin of elastocaloric effect is from the lattice softening instead of the latent heat of structural transformation [40].

Critical Stress for Martensitic Transformation, δ

The stress onset indicates the driven force in an ideal isothermal superelasticity (without stress fluctuation during transformation). The parameter δ is crucial for the specific elastocaloric properties of refrigerant materials, but even for the entire mass and volume of the elastic cooling devices. Intrinsically the value of δ is increased linearly with testing temperature above austenite finish temperature A_f. It also can be influenced by the microstructure, crystal orientation, and deformation type. Chumlyakov et al. [42] compared the δ magnitude for some single-crystalline [001]-oriented magnetic shape memory alloys (Co–Ni–Ga, Co–Ni–Al and Ni–Fe–Ga) and Ti–Ni. They found that at temperatures slightly above A_f, magnetic materials always showed much lower superelastic stress (20–40 MPa) than Ti–Ni (about 300 MPa). One can assume that δ is correlated with the twinning stress as low as 5 MPa for the rearrangement of martensitic variants. From the microstructural point of view, the martensite of magnetic shape memory alloys consists of nano-twinned modulated structure with the low twin boundary energy [43]. These particular features allow us to potentially miniaturize elastic cooling devices.

Temperature Dependence of Critical Stress, m_s

In this part, we focus on a central parameter, the sensitivity of critical stress to temperature, which now refers to $m_S = d\delta/dT$. From the well-known Clausius–Clapeyron equation:

$$\Delta S = \Delta_\varepsilon \times (d\delta/dT) \times (-1/\rho) = \Delta_\varepsilon \times m_S \times (-1/\rho), \quad (2)$$

$$\Delta T \approx (T \times \Delta S)/C_p, \quad (3)$$

where $\Delta\varepsilon$ is the transformation strain, ρ is mass density, and C_p heat capacity, the theoretical total entropy change and temperature change by stress strongly lies on the value of m_S. However, this upper limit of elastocaloric effect is only deduced from the angle of ideal conditions. In reality, the stress-induced martensitic transformation proceeds inhomogeneously, giving rise to a finite transformation width. As shown in Fig. 3a, if the value of m_S appears too large, the stress cannot fully induce the transformation and thus obviously reduces ΔT. Therefore, an optimization of m_S is highly necessary. Conversely, the complete martensitic transformation easily undergoes at the same stress for a smaller m_S. In the meantime, the stress hysteresis ($\Delta\delta$) depends on m_S too. For example, when two materials have the same transformation temperature hysteresis, the higher slope in the T-δ diagram, corresponding to the smaller m_S indicates the lower stress hysteresis, as seen in Fig. 3b. From above, we can get to know that the temperature dependence of critical stress manipulates numerous elastocaloric properties including entropy/temperature change, transformation portion, and stress hysteresis. Figure 4a displays this parameter in various magnetic and non-magnetic elastocaloric materials. To date, the physical origin of m_S is not yet very clear. It is likely ascribed to the different element formation enthalpy that leads to different temperature stability of energy barriers between martensite and austenite.

From Eq. (2), m_S is a crucial but not the solely decisive factor for ΔS and ΔT. Besides, the elastocaloric performance mainly depends on deformation orientation and transformation strain. The transformation strain $\Delta\varepsilon$ that is directly related to the lattice parameters of transformation phases, must be maximized for achieving a large elastocaloric effect. The lattice distortion can be simplified based on cubic coordinator in Heusler-type alloys, by the ratio of the short axis in tetragonal martensite to the original axis of cubic austenite, e.g., c/a_0. For example, the ductile Ni–Fe–Ga-based alloys exhibit a large $\Delta\varepsilon$ and resulting large ΔT, while Ni–Mn–Sn-based alloys show a higher m_S but much lower ΔT due to its small $\Delta\varepsilon$, as shown in Fig. 4b and c.

Irreversibility

The elastocaloric irreversibility, which refers to the difference in ΔT between loading and unloading processes due to energy losses in deformation stage [44], is a crucial parameter for elastocaloric refrigeration. To enhance the cooling capacity and reduce the energy loss of elastocaloric materials, the degree of elastocaloric reversibility should be improved. It should be noted that there are two factors

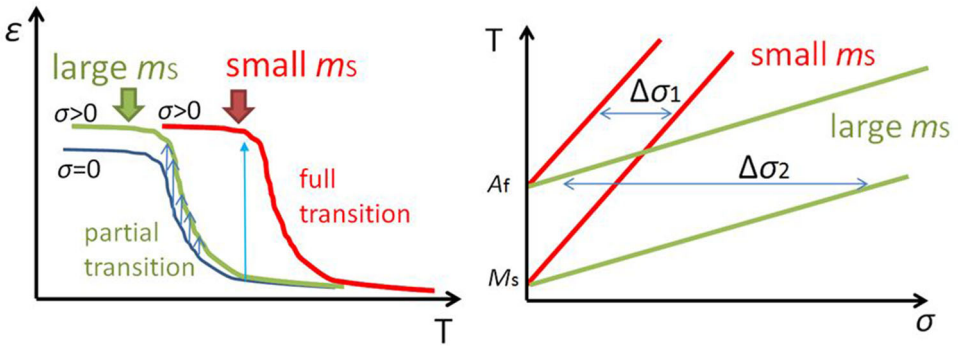

Fig. 3 *Left* the transformation strain as a function of temperature in magnetostructural transition materials with different values of the sensitivity of critical stress to temperature (mS). *Right* relationship of thermal hysteresis and stress hysteresis depending on mS

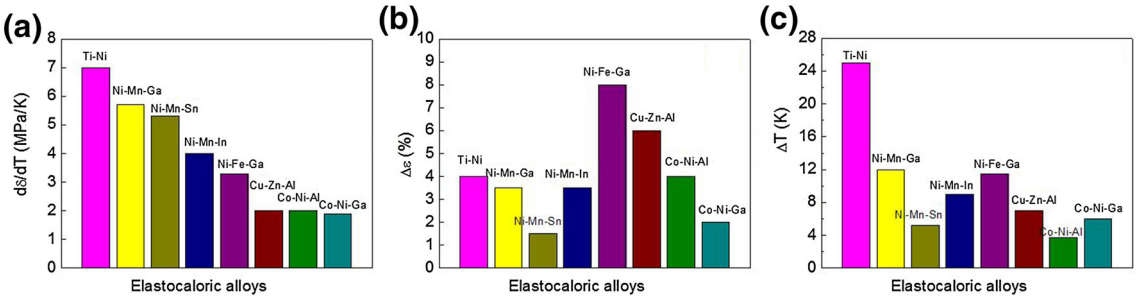

Fig. 4 Values of the sensitivity of critical stress to temperature (**a**), transformation strain (**b**), and adiabatic temperature change (**c**) for reported elastocaloric alloys

that affect the cooling efficiency and related temperature change irreversibility.

First, the stress hysteresis arising from intrinsic mechanical dissipative heat of internal friction is defined as the difference between the stress during loading and unloading stage. The stress hysteresis is primarily influenced by frictional resistance, variant interaction, and matrix strength [45]. The irreversible frictional dissipation of the interface between austenite and martensite promotes higher stress hysteresis. Frictional work is spent in overcoming resistance to interfacial motion, the resistance scales with the strength of the parent phase [46]. Likewise, the interaction between existing variants and a nucleating one in multi-variant martensitic transformation contributes an additive part to the increase of the stress hysteresis [45]. The matrix strengthening makes a negative contribution to the stress hysteresis. It is reflected by the rising slope of temperature dependence of the critical stress. Strengthening mechanisms accompanied by high elastic energy storage assists the reverse transformation and then decrease the stress hysteresis. Besides, the matrix strengthening suppresses dislocation nucleation.

The large stress hysteresis has negative effects on refrigerating efficiency and fatigue life of elastocaloric materials. As the stress hysteresis cause an entropy generation, it increases the adiabatic ΔT during loading and decreases ΔT during unloading. The reversibility of temperature change is destroyed. Meanwhile, the increased stress hysteresis increases the input work and then decreases the cooling efficiency of the refrigeration system. On the other hand, the large stress hysteresis contributes to the appearance of temporary residual strain and damages the fatigue life.

In addition to the stress hysteresis, temporary residual strain is the main source of irreversibility, which is usually encountered at high-strain-rate unloading [47]. The distinct feature of temporary residual strain is a delay in shape recovery after the mechanical stress releases. Upon fast unloading, the strain response falls behind the stress application and cannot resume immediately when the zero stress is reached. After a few minutes, as the temperature slowly rises to the ambient, the residual martensite is able to transform back to austenite and shape gradually recovers. Such residual strains could lead to a relaxation processing and destroy adiabatic condition, and thus result in a reduced temperature change during unloading.

In order to diminish the temperature irreversibility, matrix strengthening is useful for reducing the stress hysteresis. It is known that dynamic deformation conditions, temperature change, and ambient temperature also have direct impacts on both irreversibility sources [21]. It is helpful to reduce the stress hysteresis and avoid the appearance of temporary residual strain by choosing proper deformation parameters and/or slightly raising the ambient temperature [21]. Besides, enhancing the heat transfer between the specimen and ambient can eliminate the

negative impact of temperature change and decrease the irreversibility sources [44].

Ductility Improvement

From the application point of view, good ductility is desirable for the elastocaloric effect. However, the polycrystalline magnetic shape memory alloys are usually brittle, especially for Ni–Mn-based alloys. The poor ductility is one of the biggest challenges in the utilization of Ni–Mn-based alloys as refrigeration materials. In order to improve the ductility of the alloys, multiple strategies have been adopted. Because cracks prefer to initiate and propagate along the grain boundary, the strengthening of the grain boundary is an effective way. Single crystals without the grain boundary and textured polycrystalline with modified grain boundary have been prepared for elastocaloric samples with reduced brittleness [16, 18, 20, 21].

Introducing a soft phase is an idiomatic way to improve the ductility of the magnetic shape memory alloys [48–51]. The f.c.c. structure phase can be produced either by tailoring composition or post-annealing processing. Although the secondary phase inevitably hinders the magnetostructural transformation, the dual-phase Ni–Fe–Ga polycrystalline alloy with the precipitates along the grain boundaries shows much better ductility than the single-phase alloy under the precondition of an equivalent elastocaloric effect [19]. Alloying with rare-earth has been reported to be another potential way of reducing brittleness in magnetic shape memory alloys [52]. In alloys with low rare-earth content, adding the rare-earth element not only effectively refines the grain size, but also induces a rare-earth-rich phase along the grain boundaries. This combined effect leads to an apparent enhancement of the ductility of the alloys. In alloys with high rare-earth content, however, the benefits resulting from the refinement are offset by the expansion of the secondary phase. Neverthless, the newly proposed Ni–Mn–Ti magnetic shape memory alloys, which completely consisting of *d* metals, exhibit better ductility than the conventional Ni–Mn–(In,Sn,Sb) alloys which always contain main-group elements [53]. The principle of the mechanical enhancement in these new alloys has not yet been clarified.

Magneto-Volume Transitioned Materials and Barocaloric Effect

The magneto-volume effect occurs in some ferrous alloys with a large spontaneous magnetization difference across transition. In consequence, hydrostatic pressure is one of the state variables to induce metamagnetic transition and cause a barocaloric effect. As the barocaloric effect is strongly associated with the cross-correlation between the volume and magnetic order, it unnecessarily requires shear-mode martensitic transformation. Thus the selectable systems can extend from Ni–Mn-based shape memory alloys [54–56] to many other candidate materials, such as the itinerant-electron-metamagnetic La–Fe–Si–Co [57], hexagonal Mn–Co–Ge [58], $La_{0.7}Pb_{0.3}MnO_3$ manganites [59], Mn_3GaN antiperovskite [60], and ferrielectric ammonium sulfate [61]. One of the significances of barocaloric effect is that there are much less plastic deformation caused energy losses or mechanical breakdown. Also, it would be attractive to construct a bi-layer with barocaloric thin film and ferroelectric substrate. In this heterostructure, the barocaloric effect is induced by electric field [62, 63], which is very promising for the downsizing of mechanical cooling accessories for cooling tiny electronic devices.

Conclusion

To achieve the wide temperature span and high power for elastocaloric refrigeration or heat pump, the combination of large latent heat, narrow hysteresis losses, and low driven force is strongly demanded from the material point of view. The utilization of multiple fields to manipulate the magnetostructural transition allows us to in-depth understand the physical origin of magnetic lattice distortion during martensitic transformation. It is also of great importance to investigate the transformation behavior, superelastic homogeneity/stability, and elastocaloric effect for micro- and nano-scale (magnetic) shape memory foils, films and pillars, towards their novel applications.

Acknowledgements The research leading to these results has received funding from the National Natural Science Foundation of China (51771218, 51531008 and 51371184).

References

1. Goetzler W, Zogg R, Young J, Johnson C (2014) Energy Savings Potential and RDD Opportunities for Non-Vapor-Compression HVAC Technologies, prepared for U.S. Department of Energy. Navigant Consulting Inc., Chicago
2. Mañosa L, Planes A, Vives E, Bonnot E, Romero R (2009) Func. Mater. Lett. 2:73
3. Cui J, Wu YM, Muehlbauer J, Hwang YH, Radermacher R, Fackler S, Wuttig M, Takeuchi I (2012) Appl. Phys. Lett. 101:073904
4. Bonnot E, Romero R, Mañosa L, Vives E, Planes A (2008) Phys. Rev. Lett. 100:125901
5. Xie Z, Sebald G, Guyomar D (2015) Appl. Phys. Lett. 107:081905
6. Chauhan A, Patel S, Vaish R (2015) Appl. Phys. Lett. 106:172901

7. Planes A, Stern-Taulats E, Castan T, Vives E, Mañosa L, Saxena A (2015) Mater. Today 2S:S477
8. Tusek J, Enelbrecht K, Millan-Solsona R, Mañosa L, Vives E, Mikkelsen LP, Pryds N (2015) Adv. Energy Mater. 5:1500361
9. Chauhan A, Patel S, Vaish R, Bowen CR (2015) MRS Energy Sustain. 2:1
10. Qian SX, Geng YL, Wang Y, Ling JZ, Hwang YH, Radermacher R, Takeuchi I, Cui J (2016) Inter. J. Refrig. 64:1
11. Schmidt M, Kirsch S, Seekecke S, Schultze A (2016) Sci Built Environ Tech. doi:10.1080/23744731.2016.1186423
12. Mañosa L, Planes A (2017) Adv. Mater. 29:1603607
13. Soto-Parra DE, Vives E, Gonzalez-Alonso D, Mañosa L, Planes A, Romero R, Matutes-Aquino JA, Ochoa-Gamboa RA, Flores-Zuniga H (2010) Appl. Phys. Lett. 96:071912
14. Castillo-Villa PO, Soto-Parra DE, Matutes-Aquino JA, Ochoa-Gamboa RA, Planes A, Mañosa L, Gonzalez-Alonso D (2011) Phys. Rev. B 83:174109
15. Castillo-Villa PO, Mañosa L, Planes A, Soto-Parra DE, Sanchez-Llamazares JL, Flores-Zuniga H, Frontera C (2013) J. Appl. Phys. 113:053506
16. Lu BF, Xiao F, Yan AR, Liu J (2014) Appl. Phys. Lett. 105:161905
17. Lu BF, Zhang PN, Xu Y, Sun W, Liu J (2015) Mater. Lett. 148:110
18. Huang YJ, Hu QD, Bruno NM, Chen JH, Karaman I, Ross JH Jr, Li JG (2015) Scripta. Mater. 105:42
19. Xu Y, Lu BF, Sun W, Yan AR, Liu J (2015) Appl. Phys. Lett. 106:201903
20. Xiao F, Jin MJ, Liu J, Jin XJ (2015) Acta Mater. 96:292
21. Li Y, Zhao DW, Liu J (2016) Sci. Rep. 6:25500
22. Sun W, Liu J, Lu BF, Yan AR (2016) Scripta Mater. 114:1
23. Y. Li and J. Liu (unpublished data)
24. Bechtold C, Chluba C, Lima de Miranda R, Quandt E (2012) Appl. Phys. Lett. 101:091903
25. Chen X, Srivastava V, Dabade V, James RD (2013) J. Mech. Phys. Solids 61:2566
26. Chluba C, Ge WW, de Miranda RL, Strobel J, Kienle L, Quandt E, Wuttig M (2015) Science 348:6238
27. Sandeman KG (2012) Scripta Mater. 67:566
28. Liu J, Gottschall T, Skokov K, Moore JD, Gutfleisch O (2012) Nat. Mater. 11:620
29. Sanchez-Alarcos V, Recarte V, Perez-Landazabal JI, Gomez-Polo C, Rondriguez-Velamanzan JA (2012) Acta Mater. 60:459
30. Zhao P, Dai L, Cullen J, Wuttig M (2007) Metall. Mater. Trans. A 38A:745
31. Tickle R, James RD (1999) J. Magn. Magn. Mater. 195:627
32. Seiner H, Heczko O, Sedlak P, Bodnarove L, Novotny M, Kopecek J, Landa M (2013) J. Alloy. Comp. 577S:S131
33. de Launay J (1954) J. Chem. Phys. 22:1676
34. Recarte V, Perez-Landazabal JI, Sanchez-Alarcos V, Zablotskii V, Cesari E, Kustov S (2012) Acta Mater. 60:3168
35. Soto-Parra D, Vives E, Mañosa L, Matutes-Aquino JA, Flores-Zuniga H, Planes A (2016) Appl. Phys. Lett. 108:071902
36. Frenzel J, Wieczorek A, Opahle I, Maaß B, Drautz R, Eggeler G (2015) Acta Mater. 90:213
37. Stonaha PJ, Manley ME, Bruno NM, Karaman I, Arroyave R, Singh N, Abernathy DL, Chi S (2015) Phys. Rev. B 92:140406
38. Cui J, Shield TW, James RD (2004) Acta Mater. 52:35
39. Ren X, Miura N, Zhang J, Otsuka K, Tanaka K, Koiwa M, Suzuki T, Chumlyakov YI, Asai M (2001) Mater. Sci. Eng. A 312:196
40. Xiao F, Fukuda T, Kakeshita T, Jin XJ (2015) Acta Mater. 87:8
41. Xiao F, Fukuda T, Kakeshita T (2013) Appl. Phys. Lett. 102:161914
42. Chumlyakov YI, Kireeva IV, Panchenko EY, Timofeeva EE, Pobedennaya ZV, Chusov SV, Karaman I, Maier H, Cesari E, Kirillov VA (2008) Rus. Phys. J. 51:1016
43. Kaufmann S, Niemann R, Thersleff T, Roßler UK, Heczko O, Buschbeck J, Holzapfel B, Schultz L, Faehler S (2011) New. J. Phys. 13:053029
44. Tusek J, Engelbrecht K, Mikkelsen LP, Pryds N (2015) J. Appl. Phys. 117:124901
45. Hamilton RF, Sehitoglu H, Efstathiou C, Maier HJ, Chumlyakov Y (2006) Acta Mater. 54:587
46. Hamilton RF, Sehitoglu H, Chumlyakov Y, Maier HJ (2004) Acta Mater. 52:3383
47. Chen WW, Wu QP, Kang JH, Winfree NA (2001) Int. J. Solids Struct. 38:8989
48. Oikawa K, Ota T, Ohmori T, Tanaka Y, Morito H, Fujita A, Kainuma R, Fukamichi K, Ishida K (2002) Appl. Phys. Lett. 81:5201
49. Liu J, Li JG (2007) Scripta Mater. 56:109
50. Ma YQ, Yang SY, Liu Y, Liu XJ (2009) Acta Mater. 57:3232
51. Huang YJ, Hu QD, Liu J, Zeng L, Zhang DF, Li JG (2013) Acta Mater. 61:5702
52. Cai W, Gao L, Liu AL, Sui JH, Gao ZY (2007) Scripta Mater. 57:659
53. Wei ZY, Liu EK, Chen JH, Li Y, Liu GD, Luo HZ, Xi XK, Zhang HW, Wang WH, Wu GH (2015) Appl. Phys. Lett. 107:022406
54. Mañosa L, González-Alonso D, Planes A, Bonnot E, Barrio M, Tamarit JL, Aksoy S, Acet M (2010) Nat. Mater. 9:478
55. Stern-Taulats E, Planes A, Lloveras P, Barrio M, Tamarit JL, Pramanick S, Majumdar S, Yüce S, Emre B, Frontera C (2015) Acta Mater. 96:324
56. Mañosa L, Stern-Taulats E, Planes A, Lloveras P, Barrio M, Tamarit JL, Emre B, Yüce S, Fabbrici S, Albertini F (2014) Phys. Stat. Sol. B 251:2114
57. Mañosa L, González-Alonso D, Planes A, Barrio M, Tamarit JL, Titov IS, Acet M, Bhattacharyya A, Majumdar S (2011) Nat. Commun. 2:595
58. Wu RR, Bao LF, Hu FX, Wu H, Huang QZ, Wang J, Dong XL, Li GN, Sun JR, Shen FR, Zhao TY, Zheng XQ, Wang LC, Liu Y, Zuo WL, Zhao YY, Zhang M, Wang XC, Jin CQ, Rao GH, Han XF, Shen BG (2015) Sci. Rep. 5:18027
59. Kartashev AV, Mikhaleva EA, Gorev MV, Bogdanov EV, Cherepakhin AV, Sablina KA, Mikhashonok NV, Flerov IN, Volkov NV (2013) J. Appl. Phys. 113:073901
60. Matsunami D, Fujita A, Takenaka K, Kano M (2015) Nature Mater. 14:73
61. Lloveras P, Stern-Taulats E, Barrio M, Tamarit JLI, Crossley S, Li W, Pomjakushin V, Planes A, Mañosa LI, Mathur ND, Moya X (2015) Nature Commun 6:8801
62. Liu Y, Phillips LC, Mattana R, Bibes M, Barthélémy A, Dkhil B (2016) Nature Commun. 7:11614
63. Gong YY, Wang DH, Cao QQ, Liu EK, Liu J, Du YW (2015) Adv. Mater. 27:801